Stochastic Modeling of a Fluidized-Bed Reactor

J. R. TOO

Department of Chemical Engineering
The Catholic University of America
Washington, DC 20064

R. O. FOX, L. T. FAN and R. NASSAR

Department of Chemical Engineering
Kansas State University
Manhattan, KS 66506

In this work dispersive mixing and chemical reactions are treated simultaneously by resorting to the theory of stochastic processes. A fluidized-bed reactor is modeled by discretizing it into ideally stirred tanks of various sizes corresponding to bubble, cloud, and emulsion phases. All parameters in the model are correlated with known or experimentally obtainable quantities. Examples using a complex chemical reaction are given to demonstrate the applicability of the approach.

SCOPE

One of the readily observable features of the flow pattern in a gas-solids, fluidized-bed reactor is its fluctuating characteristics. Such a reactor is often visualized as containing at least two distinct phases, namely the dense (emulsion) and dilute (bubble) phases (Kato and Wen, 1969; Mori and Wen, 1975, 1976; Peters et al., 1982; Orcutt and Carpenter, 1971). The flow patterns of gas and solids in and around these phases fluctuate constantly and the various components in the dense phase are intermittently exposed to bubbles of different gas compositions. It is thus natural that we resort to a probabilistic approach to gain insight into such a system (Krambeck et al., 1969; Ligon and Amundson, 1981). In their study of fluidized-bed reactors, Bukur et al. (1977) have stated, "It is our view that probably no deterministic model will ever describe such reactors with any precision. While some stochastic models have been proposed, no serious work in this direction has been presented."

The theory of the Markov process (continuous time Markov chain) has been successfully used for modeling and simulating totally interconnected stirred-tank networks. It has been recognized that a fluidized-bed reactor can be discretized into ideally stirred tanks of various sizes corresponding to bubble, cloud, and emulsion phases. The bubble assemblage model (BAM) proposed by Kato and Wen (1969) is an example. In the present work, the theory of the Markov process is employed for modeling dispersive mixing and chemical reactions simultaneously in such a reactor.

The bubble assemblage model has been shown to be one of the most useful models proposed for a bubbling, gas-solids, fluidized-bed reactor. An essential feature of this model is that the bed is divided into compartments whose heights are adjusted to the bubble sizes at that level. This greatly reduces computing time without loss of accuracy.

In this paper we shall only deal with heterogenous catalytic reactions in which the time history of solids is not important. All parameters of the model are correlated with known or experimentally obtainable quantities. Examples using a complex chemical reaction are given to demonstrate the applicability of the approach.

CONCLUSIONS AND SIGNIFICANCE

In this work a stochastic compartmental model has been introduced for gaseous fluidized-bed reactors which takes into account both flow reversal and the height of the entering jets in addition to all other phenomena contained in previous deterministic models. The resultant formulation yields not only the mean concentrations of reacting species in each compartment, but also the expressions for the variance and higher-order cumulants.

The proposed stochastic model has been applied to simulation of fluidized-bed reactors involving a complex reaction under various flow conditions. The axial concentration profiles as well as the transient exit concentrations have been determined directly from the transition probability matrix and initial conditions. The results show that even under nonslugging conditions, flow reversal will not commonly occur within the range of the governing equations; however the magnitude of crossflow between the bubble and emulsion phases has been found to be a more significant factor determining the axial concentration profile in the fluidized-bed reactor at steady state. It has also been found that inclusion of the jet height in calculating the number of idealized compartments influences the performance of the reactor appreciably, especially at low superficial gas velocities. Nevertheless, further investigation needs to be carried out to determine the relationship between the bed diameter and flow reversal conditions.

Each of the reactor systems considered here involves an exceedingly large number of randomly behaving entities, namely molecules; thus the stochastic model yields results identical to those obtained by means of a deterministic mass balance ap-

Correspondence concerning this paper should be addressed to L. T. Fan.
R. Nassar is with the Department of Statistics, Kansas State University.

proach. The use of the stochastic approach, however, reduces manipulative and computational efforts for formulating and solving the model equations. Furthermore, the use of the stochastic approach tends to provide additional insight into the system. For a reactor in which a small number of reacting entities are present, a stochastic formulation offers additional information since the variance of the concentration and higher-order cumulants can also be determined. An example of such a system is a fluidized-bed coal combustor where the diameter of burning coal particles may exceed 1 cm. A stochastic formulation therefore offers a viable alternative to the deterministic approach.

STOCHASTIC MODEL

The theory presented here is mainly based on our previous work (Fan et al., 1982; Nassar et al., 1981, 1982). Consider a fluidized-bed reactor with m interconnected compartments consisting of two phases. The volumes of the compartments are not necessarily identical. Suppose that entities or molecules of types, $A_1, A_2, \ldots, A_n$, enter the reactor through the first compartment and leave it through the last compartment. Also suppose that linear transitions take place among the entities or molecules in the reactor.

In each compartment, an entity or molecule of type A_i may transfer to another type due to chemical reactions, remain in its present state, move to the other phase in the same compartment, move to another compartment, or exit from the reactor if this compartment is the last one. For a reactor with m compartments, n types of entities, and two phases, we have a Markov process with a sample space of $2mn$ states. The states may be designated as $S_1, S_2, \ldots, S_{2mn}$, where $\{S_1, S_2, \ldots, S_n\}$ represents the set of states in phase 1 of compartment 1, $\{S_{n+1}, S_{n+2}, \ldots, S_{2n}\}$ the set in phase 1 of compartment 2, and so on. Formally, we let

$p_{ij}(t,t+\Delta t)$
$= Pr$ [an entity or molecule in state S_i at time t will be in state S_j $(j \neq i)$ at time $(t+\Delta t)$].
$= k_{ij}(t)\Delta t + o(\Delta t)$ (1)

and

$p_{id}(t,t+\Delta t)$
$= Pr$ [an entity or molecule in state S_i (in the top compartment) at time t will exit from the reactor at time $(t+\Delta t)$]
$= \mu_i(t)\Delta t + o(\Delta t)$ (2)

Here $k_{ij}(t)$ and $\mu_i(t)$ are the so-called intensity functions of the Markov process. Obviously,

$$\sum_{j=1}^{2mn} p_{ij}(t,t+\Delta t) + p_{id}(t,t+\Delta t) = 1 \tag{3}$$

Let

$$p_{ii}(t,t+\Delta t) \equiv 1 + k_{ii}(t)\Delta t + o(\Delta t) \tag{4}$$

Then, from Eqs. 1 through 4, we have

$$k_{ii}(t) = -\left[\sum_{j \neq i} k_{ij}(t) + \mu_i(t)\right] \tag{5}$$

The intensity function $\{k_{ij}(t)\}$ within a phase may be interpreted as rate constants for linear first-order reactions (Ishida, 1960; Nassar et al., 1981). The intensity functions between states in two different compartments, or between phases in the same compartment, may be interpreted as the rate of migration or movement of entities between the two compartments or phases. If these intensity functions are time-independent, the process is said to be a time-homogeneous process. Otherwise it is a time-heterogeneous process.

For a time interval (τ,t), we define

$p_{ij}(\tau,t)$ = probability that an entity or molecule in state S_i at time τ will be in state S_j at time t, $i,j = 1, 2, \ldots, 2mn$

Let $\boldsymbol{P}(\tau,t)$ be the matrix of transition probabilities $[p_{ij}(\tau,t)]$. It has been shown that these transition probabilities satisfy the Kolmogorov forward differential equations (Chiang, 1980), i.e.,

$$\frac{d}{dt}\boldsymbol{P}(\tau,t) = \boldsymbol{P}(\tau,t)\boldsymbol{K}(t) \tag{6}$$

with the initial condition

$$\boldsymbol{P}(\tau,t) = \boldsymbol{I} = \text{identity matrix @ } t = \tau \tag{7}$$

The matrix $\boldsymbol{K}(t)$ in Eq. 6 is the so-called intensity matrix defined as $\boldsymbol{K}(t) = [k_{ij}(t)]$.

For the time-homogeneous process the forward differential equation, Eq. 6, becomes

$$\frac{d}{dt}\boldsymbol{P}(t-\tau) = \boldsymbol{P}(t-\tau)\boldsymbol{K} \tag{8}$$

with the initial condition $\boldsymbol{P}(0) = \boldsymbol{I}$.

The solutions of Eqs. 6 and 8 for the transition probabilities, $\{p_{ij}(\tau,t)\}$ and $\{p_{ij}(t-\tau)\}$, are given in standard treatises on stochastic processes or ordinary differential equations (Chiang, 1980; Bellman, 1960). With these transition probabilities known, we can obtain the mean and variance of the number of any type of entity in each compartment and phase in the fluidized-bed reactor even under time-heterogeneous conditions, including those prevailing in unsteady state operations (Fan et al., 1982). For instance, we let f_1 and f_{2m} be the number of entities of the reactant entering the

TABLE 1. SUMMARY OF PARAMETER ESTIMATION

$$L = L_{mf}\left[\frac{(U_o - U_{mf}) + 0.71\sqrt{gD_b}}{(U_o - U_{mf}) + 0.71\sqrt{gD_b} - \Upsilon(U_o - U_{mf})}\right]$$

$$\overline{D}_b = D_{bm} - [(D_{bm} - D_{bo})\exp(-0.15L_{mf}/D_R)]$$

$$\Upsilon = 0.7585 - 0.0013(U_o - U_{mf}) + 0.0005(U_o - U_{mf})^2$$

$$D_{bm} = 0.652[A(U_o - U_{mf})]^{0.4}$$

$$D_{bo} = 0.347\left[\frac{A}{N_D}(U_o - U_{mf})\right]^{0.4}$$

$$h_j = \frac{d_p}{0.0007 + 0.556d_p}\left[\frac{A}{N_D}(U_o - U_{mf})\right]^{0.35}$$

$$h_c = \frac{D_R}{0.3}\ln\left[\frac{D_{bm} - D_{bo}}{D_{bm} - D_{bc}}\right]$$

$$\Delta h_p = \frac{D'_{bp}}{1 + 0.15(D'_{bp} - D_{bm})/D_R}$$

$$D_{bp} = D_{bm} - (D_{bm} - D_{bo})\exp[-0.3(h_p - h_f)/D_R]$$

$$U_{bp} = (U_o - U_{mf}) + 0.71\sqrt{gD_{bp}}$$

$$\beta_p = \left(\frac{\epsilon_{mf}U_{bp}}{\epsilon_{mf}U_{bp} - U_{mf}}\right)^{1/3}$$

$$\epsilon_{bp} = \frac{U_o - U_{mf}}{0.71\sqrt{gD_{bp}}}$$

$$\delta_{cp} = \frac{3U_{mf}}{0.71\epsilon_{mf}\sqrt{gD_{bp}} - U_{mf}}$$

$$V_{bp} = \epsilon_{bp}A\Delta h_p(1 - \delta_{cp})$$

$$V_{ep} = \Delta h_p A - V_{bp}$$

$$\delta_{bp} = \frac{V_{bp}}{AD_{bp}\beta_p}$$

$$U_{bsp} = (U_{bp} + 1.33U_{mf})\delta_{bp}$$

$$F^{\ell}_{bep} = \frac{2.0U_{mf}}{D_{bp}} + 6.78\left(\frac{\mathcal{D}^{\ell}_p\epsilon_{mf}U_{bp}}{D^3_{bp}}\right)^{0.5}$$

$$G_{bep} = U_{bsp} - U_{bsp-1}$$

$$G_{be1} = 0$$

$$U_{esp} = U_o - U_{bsp}$$

fluidized bed through the bubble and emulsion phases of compartment 1 per unit time, respectively, for the case of one reactant. Then, the mean and variance of the number of entities in the bubble phase of compartment p are, respectively,

$$E[x_p] = \int_0^t [f_1 p_{1,p}(t-\tau) + f_{2m} p_{2m,p}(t-\tau)]d\tau \quad (9)$$

$$\mathrm{Var}[x_p] = \int_0^t \{f_1 p_{1,p}(t-\tau)[1 - p_{1,p}(t-\tau)] + f_{2m} p_{2m,p}(t-\tau)[1 - p_{2m,p}(t-\tau)]\}d\tau \quad (10)$$

where $p_{ij}(t-\tau)$ is found from the solution of Eq. 8, and $x_p = c^l_{b_p} V_{b_p} N_A$.

ESTIMATION OF PARAMETERS

A complete description of all necessary parameter estimations is beyond the scope of this work. The relationships used in this model for the estimations are summarized in Table 1.

To estimate the values of the elements k_{ij} of the intensity matrix, it is necessary first to calculate the volumes and number of the compartments, and second to calculate gas flow rates between compartments and between phases. An example element k_{ij} representing the transitions from the bubble phase to the emulsion phase would then equal

$$k_{ij} = \frac{\text{total volumetric flow of gas from the bubble phase to the emulsion phase}}{\text{volume of gas in the bubble phase}}$$

All other elements are found analogously.

The present stochastic model parallels the deterministic model presented by Peters et al. (1982) wherein the material balance equations for reacting species ℓ in both phases of compartment p of the m compartments are written as follows.

Bubble Phase

$$V_{b_p}\frac{dC^\ell_{b_p}}{dt} = U_{bs_{p-1}} A C^\ell_{b_{p-1}} - U_{bs_p} A C^\ell_{b_p} + G_{be_p} A C^\ell_{e_p} + F^\ell_{be_p} V_{b_p}(C^\ell_{e_p} - C^\ell_{b_p}) \quad (11)$$

for compartment p where

$$1 \le p \le m.$$

Emulsion Phase

$$\epsilon_{mf} V_{e_p}\frac{dC^\ell_{e_p}}{dt} = U_{es_{p-1}} A C^\ell_{e_{p-1}} - U_{es_p} A C^\ell_{e_p} - G_{be_p} A C^\ell_{e_p} - F^\ell_{be_p} V_{b_p}(C^\ell_{e_p} - C^\ell_{b_p}) + V_{e_p}\eta^\ell_{e_p} \quad (12)$$

for compartment p where

$$U_{es_{p-1}} \ge 0$$
$$U_{es_p} \ge 0,$$

$$\epsilon_{mf} V_{e_p}\frac{dC^\ell_{e_p}}{dt} = |U_{es_p}| A C^\ell_{e_{p+1}} + U_{es_{p-1}} A C^\ell_{e_{p-1}} - G_{be_p} A C^\ell_{e_p} - F^\ell_{be_p} V_{b_p}(C^\ell_{e_p} - C^\ell_{b_p}) + V_{e_p}\eta^\ell_{e_p} \quad (13)$$

for compartment p where

$$U_{es_{p-1}} \ge 0$$
$$U_{es_p} \le 0,$$

$$\epsilon_{mf} V_{e_p}\frac{dC^\ell_{e_p}}{dt} = U_{es_{p-1}} A C^\ell_{e_p} - U_{es_p} A C^\ell_{e_{p+1}} - G_{be_p} A C^\ell_{e_p} - F^\ell_{be_p} V_{b_p}(C^\ell_{e_p} - C^\ell_{b_p}) + V_{e_p}\eta^\ell_{e_p} \quad (14)$$

for compartment p where

$$U_{es_p} \le 0$$
$$U_{es_{p-1}} \le 0,$$

and

$$\epsilon_{mf} V_{e_p}\frac{dC^\ell_{e_p}}{dt} = U_{es_{p-1}} A C^\ell_{e_p} - U_{es_p} A C^\ell_{e_p} - G_{be_p} A C^\ell_{e_p} - F^\ell_{be_p} V_{b_p}(C^\ell_{e_p} - C^\ell_{b_p}) + V_{e_p}\eta^\ell_{e_p} \quad (15)$$

for compartment p where

$$U_{es_p} \ge 0$$
$$U_{es_{p-1}} \le 0$$

From these relations the intensity matrix elements can be derived.

In this work the heights of the compartments have been determined using the method outlined by Mori and Wen (1976). The height of the first compartment, Δh_1, has been estimated by calculating the height of the jetting gas, h_j, and adding the correction factor, h_c, to this value as follows:

$$\Delta h_1 = h_j + h_c \quad \text{if } h_c > 0 \quad (16)$$

and

$$\Delta h_1 = h_j + D_{b_o} \quad \text{if } h_c = 0 \quad (17)$$

The heights of the remaining compartments are then calculated based on the equivalent spherical bubble diameter at the top of the preceding compartment. Further details can be found in the original work by Mori and Wen (1976). Using this method the bed can be divided into m compartments; the height of each compartment above the distribution plate is taken to be the same as the height of the center of the compartment above the distributor. Once the number and heights of the compartments have been determined, the volume of the bubble phase, V_{b_p}, and that of the emulsion phase, V_{e_p}, in each compartment can be found.

To determine the elements of the intensity matrix along the axial direction it is also necessary to have superficial gas velocities through both phases in each compartment. For the bubble phase this is U_{bs_p}, and for the emulsion phase U_{es_p}. The elements of the intensity matrix are then equal to the volumetric flow rate, $U_{bs_p}A$ or $U_{es_p}A$, divided by the volume of gas in the phase. This yields

$$k^b_{p,p+1} = \frac{U_{bs_p} A}{V_{b_p}}, \quad (18)$$

for the bubble phase and

$$k^e_{p,p+1} = \frac{U_{es_p} A}{\epsilon_{mf} V_{e_p}}, \qquad U_{es_p} > 0 \quad (19)$$

or

$$k^e_{p,p-1} = \frac{U_{es_{p-1}} A}{\epsilon_{mf} V_{e_p}}, \qquad U_{es_p} < 0 \quad (20)$$

for the emulsion phase.

To determine the intensity matrix elements between the two phases at the same axial position of the bed it is necessary to have magnitudes of the flow rates across the phase boundaries. From the material balance equations we find that the flow rate from the bubble phase to the emulsion phase in $F^\ell_{be_p} V_{b_p}$, and from the emulsion to the bubble phase is $(G_{be_p} A + F^\ell_{be_p} V_{b_p})$.

The intensity matrix elements for horizontal mixing when G_{be_p} is nonnegative are

$$k^\ell_{be_p} = F^\ell_{be_p}, \quad (21)$$

for flow from the bubble phase to the emulsion phase, and

$$k^\ell_{eb_p} = \frac{G_{be_p} A + F^\ell_{be_p} V_{b_p}}{\epsilon_{mf} V_{e_p}}, \quad (22)$$

for the flow from the emulsion phase to the bubble phase in compartment p. If G_{be_p} is negative, indicating a flow in the reverse direction, then

$$k^\ell_{be_p} = F^\ell_{be_p} + \frac{|G^\ell_{be_p}| A}{V_{b_p}} \quad (23)$$

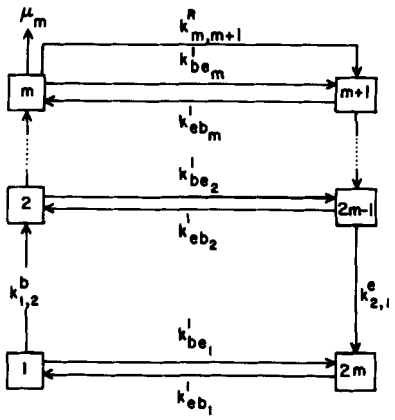

Figure 1. Example gas flow pattern and corresponding transition matrix elements.

and

$$k_{eb_p} = \frac{F_{be_p} V_{b_p}}{\epsilon_{mf} V_{e_p}} \tag{24}$$

To complete the intensity matrix it is also necessary to have the intensities of exit, μ_m and μ_{m+1}, from the top compartment and/or the recycle flow rate in the top compartment. These can be determined using a material balance around the top compartment. The intensity of exit from the bubble phase will then be

$$\mu_m = \frac{q^b_{ex}}{V_{b_m}}, \qquad q^b_{ex} > 0 \tag{25}$$

where q^b_{ex} is the volumetric flow rate of the exit stream from the bubble phase. The intensity of exit for the emulsion phase is

$$\mu_{m+1} = \frac{q^e_{ex}}{\epsilon_{mf} V_{e_m}}, \qquad q^e_{ex} > 0 \tag{26}$$

where q^e_{ex} is the volumetric flow rate of the exit stream from the emulsion phase; naturally, $q^b_{ex} + q^e_{ex} = U_o A$. If either q^b_{ex} or q^e_{ex} is greater than $U_o A$, then there is a recycle stream from the bubble phase to the emulsion phase or from the emulsion phase to the bubble phase, respectively. In this case the recycle stream will contribute an intensity matrix element for the flow between the bubble and emulsion phases in the top compartment of the form

$$k^R_{m,m+1} = \frac{q^b_{ex} - U_o A}{V_{b_m}}, \qquad q^b_{ex} > U_o A \tag{27}$$

$$k^R_{m+1,m} = \frac{q^e_{ex} - U_o A}{\epsilon_{mf} V_{e_m}}, \qquad q^e_{ex} > U_o A \tag{28}$$

The intensity matrix can then be formulated for the system. For the flow pattern shown in Figure 1, some of the example elements for the one-component (no reaction) system are

$$k_{1,2} = k^b_{1,2} \tag{29}$$

$$k_{1,2m} = k^l_{be_1} \tag{30}$$

$$k_{2,2m-1} = k^l_{be_2} \tag{31}$$

$$k_{m,m+1} = k^R_{m,m+1} + k^l_{be_m} \tag{32}$$

$$k_{m+1,m} = k^l_{eb_m} \tag{33}$$

$$k_{2m-1,2} = k^l_{eb_2} \tag{34}$$

$$k_{2m-1,2m} = k^e_{2,1} \tag{35}$$

$$k_{2m,1} = k^l_{eb_1} \tag{36}$$

$$k_{1,1} = -(k^b_{1,2} + k^l_{be_1}) \tag{37}$$

$$k_{m,m} = -(k^R_{m,m+1} + k^l_{be_m} + \mu_m) \tag{38}$$

$$k_{2m,2m} = -k^l_{eb_1} \tag{39}$$

TABLE 2. VALUES OF INPUT PARAMETERS FOR EXAMPLES

$\epsilon_{mf} = 0.5$
$D_R = 30.0$ cm
$N_D = 60$
$d_p = 0.010$ cm
$\mathcal{D}^A = \mathcal{D}^B = \mathcal{D}^C = 0.18$ cm^2/s
$C^A_o = 1.0$ gmol/cm^3
$C^B_o = C^C_o = 0.0$ gmol/cm^3
$C^A_l = C^B_l = C^C_l = 0.0$ gmol/cm^3
$k_1 = 50$/s
$k_2 = 1$/s

The intensity function k_{ij} for the chemical reactions, which take place only in the emulsion phase for a solid-catalyzed reaction, is of the form

$$k_{ij} = \eta^{\ell}_{e_p} \tag{40}$$

The intensity matrix for the emulsion phase in one compartment wherein a two-component reaction takes place is of the form (Fan et al., 1982)

$$U_{ij} = \begin{bmatrix} k_{p,p} & \eta^1_{e^p} \\ \eta^2_{e^p} & k_{p+1,p+1} \end{bmatrix} \tag{41}$$

where

$$X_1 \underset{\eta^2_{e^p}}{\overset{\eta^1_{e^p}}{\rightleftarrows}} X_2$$

RESULTS AND DISCUSSION

As an example of complex chemical reactions, the series reactions

$$A \xrightarrow{k_1} B \xrightarrow{k_2} C$$

are considered. The values of input parameters employed are listed in Table 2. Variations of both density and molecular diffusion are neglected; that is,

$$\rho^A = \rho^B = \rho^C \tag{42}$$

and

$$\mathcal{D}^A = \mathcal{D}^B = \mathcal{D}^C \tag{43}$$

For the three-component system under consideration, the intensity matrix has $6m$ rows and columns. For the superficial gas velocities used in the examples shown in Figures 2 through 7 and bed parameters listed in Table 2, the resultant intensity matrices are 24 × 24 square matrices. Solving Eq. 8 with these intensity matrices yields the transition probabilities as functions of time. The

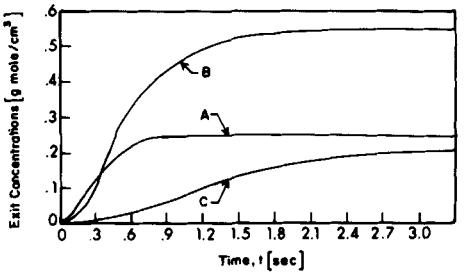

Figure 2. Transient exit concentrations: U_o = 40.0 cm/s; U_{mf} = 1.0 cm/s; L_{mf} = 20.0 cm.

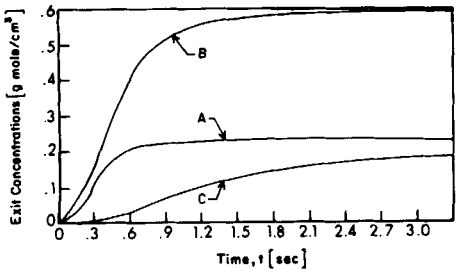

Figure 3. Transient exit concentrations: U_o = 45.0 cm/s; U_{mf} = 2.0 cm/s; L_{mf} = 15.0 cm.

mean and variance of the concentration can be found for each component in each compartment from these probabilities according to Eqs. 9 and 10. The variance of the concentration is not shown; it is equal to the concentration in compartment i divided by the volume of compartment i and the Avogadro number. For a system where the reacting species are subdivided into essentially molecular scale groupings, the variance will be insignificant relative to the average concentration. However in a system where molecules of the reacting species are lumped into finite size groups that move together—e.g., particles of coal in a gasifier or reactant molecules in the dispersed phase of a liquid-liquid reactor—the Avogadro number must be replaced by an appropriate number representing the number of individual entities in a characteristic unit, which is often substantially smaller than the former. For such a system the variance of the concentration may not be negligible relative to the average concentration since the number of independently behaving entities is relatively small. For example, for a system wherein 100 μm particles are involved in a chemical reaction, the number of particles that can be packed into a one-liter compartment will be in the order of 10^9 particles. If the Avogadro number is replaced by this number, the variance will be of the order of 10^{-9}. The maximum number of particles that can be suspended in the gas phase passing through the compartment would be much smaller than 10^9 and therefore the variance would increase accordingly. Other systems, such as rarified gas reactions, reactions inside catalyst particles, and microbial reactors, all of which involve relatively small numbers of reacting entities, would also be expected to exhibit appreciable variances which should not be neglected.

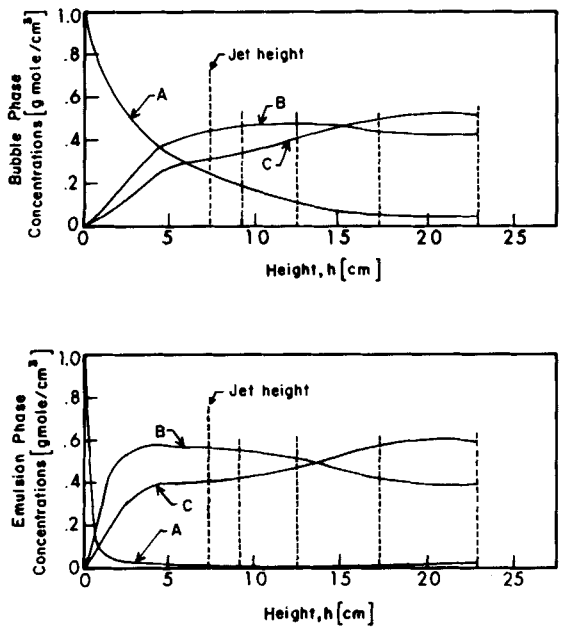

Figure 4. Axial concentration profiles: U_o = 7.5 cm/s; U_{mf} = 1.0 cm/s; L_{mf} = 20.0 cm. Dotted lines indicate compartment heights; the corresponding flow pattern is shown in Figure 8a.

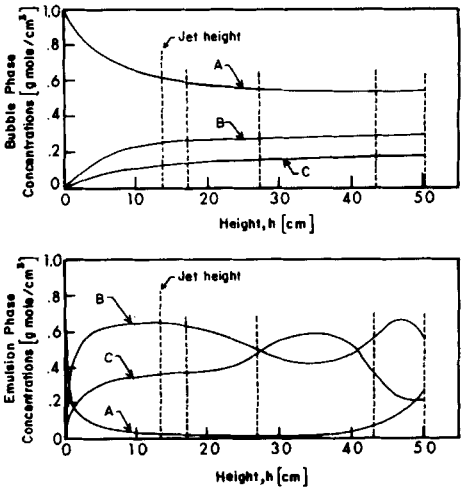

Figure 5. Axial concentration profiles: U_o = 40.0 cm/s; U_{mf} = 1.0 cm/s; L_{mf} = 20.0 cm. Dotted lines indicate compartment heights; the corresponding flow pattern is shown in Figure 8b.

Transient Exit Concentrations

As done by Peters et al. (1982), we have calculated the transient exit concentration, as shown in Figures 2 and 3, for each of the three reacting species for the given values of U_o, U_{mf}, and L_{mf}. These concentrations have been evaluated by averaging over the concentrations in both phases of the top compartment using the exit flow rates, q^e_{ex} and q^b_{ex}.

A minor difference exists between Figures 2 and 3. In Figure 2 the concentration of component A is initially greater than that of component B before falling to approximately the level shown in Figure 3. In Figure 3 the concentration of component B is greater than that of component A for all times. This is of questionable significance, however, since stirred-tanks-in-series models do not necessarily predict transient behavior accurately.

Axial Concentration Profiles

Figures 4 through 7 show typical steady state axial concentration profiles for each of the three species for the given values of U_o, U_{mf}, and L_{mf}. The corresponding gas flow pattern in the bed for Figures 4, 6, and 7 is shown in Figure 8a, and that for Figure 5 in

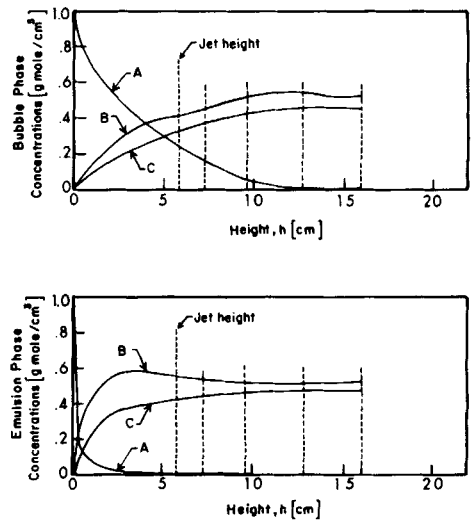

Figure 6. Axial concentration profiles: U_o = 5.5 cm/s; U_{mf} = 2.0 cm/s; L_{mf} = 15.0 cm. Dotted lines indicate compartment heights; the corresponding flow pattern is shown in Figure 8a.

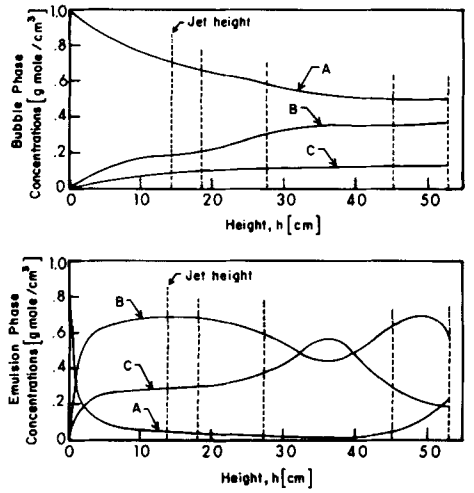

Figure 7. Axial concentration profiles: U_o = 45.0 cm/s; U_{mf} = 2.0 cm/s; L_{mf} = 15.0 cm; Dotted lines indicate compartment heights; the corresponding flow pattern is shown in Figure 8a.

Figure 8b. The difference between the two cases given in Figure 8 is that flow reversal occurs only in one example (Figures 5 and 8b). In Figures 4 through 7 discrete stepwise curves resulting from the discretization of the bed are replaced with smooth curves drawn through the average concentration in each section. Comparison of Figures 5 and 7 with Figures 4 and 6, respectively, indicates that the conversion of component A is significantly decreased with an increase in the superficial gas velocity U_o due to bypassing of the emulsion phase or reaction zone through the bubble phase. Perhaps a more significant result is seen when comparing Figures 5 and 7. The gas flow pattern in Figure 5 is shown in Figure 8b, where it is seen that there is a flow reversal in the upper compartments in the emulsion phase. The gas flow pattern corresponding to Figure 7, given in Figure 8a, shows no flow reversal. However the axial concentration profiles shown in Figures 5 and 7 are qualitatively identical, suggesting that flow reversal has little effect on conversion for the solid-catalyzed reaction studied here.

The question arises as to the origin of the S-shaped axial concentration profiles seen in Figures 5 and 7 for components B and C. Close scrutiny seems to suggest that the crossflow, G_{be_p}, not the flow reversal (Peters, 1982), is the governing factor. The relatively large values of G_{be_p} in the top compartment correspond to flow of a significant amount of unreacted component A from the bubble phase to the emulsion phase; component A reacts eventually in the latter, thus increasing the concentration of component B in it. The crossflow term in the top compartment is much greater than the upward or downward superficial gas velocity through the emulsion phase in the top compartment. This results in a maximum

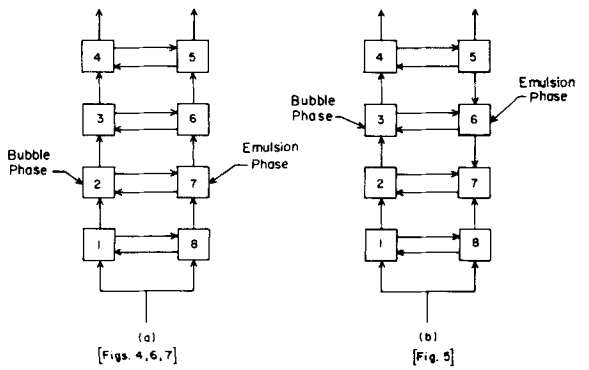

Figure 8. Gas flow patterns for the examples: (a) without flow reversal; (b) with flow reversal.

in the concentration profile of component C in the emulsion phase of the third compartment which corresponds to box 6 in Figures 8a and b. The occurrence of this maximum in the concentration profile of component C persists for increasing superficial gas velocities; this is totally independent of the onset of flow reversal.

Flow Reversal

Another interesting aspect, revealed through simulations for several different sets of the operating parameters, is that flow reversal conditions are the exception rather than the rule according to the present model. In most cases slugging would occur before onset of flow reversal, or no flow reversal is found within the feasible ranges of equations used in the parameter estimation.

Effect of Jet Height

Simulations for wide ranges of the operating parameters have indicated that inclusion of the jet height as a parameter in determining the size of the first compartment has a significant effect on the number of compartments necessary in modeling the bed at relatively low superficial gas velocities, U_o. Under such conditions the necessary number of compartments is reduced due to the predominance of the jetting gas. For values of U_o in the middle of the feasible range, the number of necessary compartments increases as the bed height increases; it falls when U_o is further increased as the bubble size increases and becomes the dominating parameter.

ACKNOWLEDGMENT

This work was conducted under the sponsorship of the Engineering Experiment Station (Kansas Energy Project) of Kansas State University.

NOTATION

A = cross-sectional area of bed, cm^2
$C_{b_p}^{\ell}$ = gas concentration of species ℓ in bubble phase in compartment p, gmol/cm^3
C_o^{ℓ} = gas concentration of species ℓ in entire fluidized bed at start, gmol/cm^3
$C_{e_p}^{\ell}$ = gas concentration of species ℓ in emulsion phase in compartment p, gmol/cm^3
C_f^{ℓ} = gas concentration of species ℓ in inlet stream, gmol/cm^3
d_p = diameter of holes in distributor plate, cm
D_R = reactor diameter, cm
D_{b_p} = equivalent spherical bubble diameter having the same volume as a bubble, cm
D_{b_m} = maximum bubble diameter, cm
D_{b_o} = initial bubble diameter, cm
D_{b_p} = D_{b_p} evaluated at boundary between compartments $(p-1)$ and p, cm
$\overline{D}_b$ = average equivalent bubble diameter, cm
f_i = flowrate of entities from environment into state S_i, number/s
$F_{be_p}^{\ell}$ = gas interchange coefficient for species ℓ from bubble phase to emulsion phase in compartment p per unit volume of bubble phase, 1/s
g = gravitational acceleration, cm/s^2
G_{be_p} = crossflow from bubble phase to emulsion phase, cm/s
h = height above distribution plate, cm
h_p = height of compartment p from distributor plate, cm
Δh_p = height of compartment p, cm
h_j = height of entering jets, cm
h_c = critical height from top of jets where value of ϵ_c becomes equal to ϵ_c^* or 0.6, cm

$k_{i,j}$ = intensity of transition between states S_i and S_j, 1/s
k_1, k_2 = reaction rate constants, 1/s
$k^b_{p,p+1}$ = intensity of transition between compartments p and $(p+1)$ for bubble phase, 1/s
$k^e_{p,p+1}$ = intensity of transition between compartments p and $(p+1)$ for emulsion phase, 1/s
$k^e_{p,p-1}$ = intensity of transition between compartments p and $(p-1)$ for emulsion phase, 1/s
$k^\ell_{be_p}$ = intensity of transition from bubble phase to emulsion phase for species ℓ in compartment p, 1/s
$k^\ell_{eb_p}$ = intensity of transition from emulsion phase to bubble phase for species ℓ in compartment p, 1/s
$k^R_{m+1,m}$ = intensity of transition from emulsion phase to bubble phase in top compartment for recycle, 1/s
K = intensity matrix = $[k_{ij}]$
L = expanded bed height, cm
L_{mf} = bed height at U_{mf}, cm
N_A = Avogadro number, 1/gmol
N_D = number of holes in distributor plate
$P_{ij}(t)$ = transition probability that a molecule in state S_i at time 0 will be in state S_j at time t
t = time, s
U_{b_p} = linear bubble phase gas velocity in compartment p, cm/s
U_o = superficial gas velocity, cm/s
U_{mf} = minimum fluidization velocity, cm/s
U_{bs_p} = superficial gas velocity in bubble phase in compartment p, cm/s
U_{es_p} = superficial gas velocity in emulsion phase in compartment p, cm/s
V_{b_p} = volume of bubble phase in compartment p, cm^3
V_{e_p} = volume of emulsion phase in compartment p, cm^3
x_i = number of entities in state S_i
Y = parameter defined in Table 1
$\mathcal{D}^\ell_p$ = molecular diffusion coefficient of species ℓ in compartment p, cm^2/s

Greek Letters

ϵ_c = void fraction of bubble phase including associated cloud
ϵ_{mf} = void fraction of bed at U_{mf}
ϵ_{b_p} = void fraction of bubble phase in compartment p
β_p = parameter defined in Table 1
δ_{c_p} = ratio of cloud volume to volume of bubble in compartment p
ρ^ℓ = molar density of species ℓ, gmol/cm^3
$\eta^\ell_{e_p}$ = reaction rate constant for species ℓ in compartment p, 1/s
μ_m = intensity of exit from the bubble phase in top compartment, i.e., compartment m, 1/s
μ_{m+1} = intensity of exit from emulsion phase in top compartment, i.e., compartment m, 1/s

Subscripts

m = final compartment
p = compartment number

Superscripts

ℓ = species
p = compartment number

LITERATURE CITED

Bellman, R., *Introduction to Matrix Analysis*, McGraw-Hill, New York (1960).

Bukur, D., H. S. Caram, and N. R. Amundson, "Some Model Studies of Fluidized Bed Reactors," *Chemical Reactor Theory: A Review*, L. Lapidus and N. R. Amundson, Eds., Prentice-Hall, Englewood Cliffs, NJ (1977).

Chiang, C. L., *An Introduction to Stochastic Processes and Their Applications*, Krieger, New York (1980).

Fan, L. T., J. R. Too, and R. Nassar, "Stochastic Flow Reactor Modeling: A General Continuous Time Compartment Model with First-Order Reactions," *Residence Time Distribution Theory in Chemical Engineering*, A. Pethö and R. D. Noble, Eds., Verlag Chemie, Weinheim, West Germany (1982).

Ishida, K., "The Stochastic Model for Unimolecular Gas Reaction," *Bull. Chem. Soc. Japan*, **33**, 1,030 (1960).

Kato, K., and C. Y. Wen, "Bubble Assemblage Model for Fluidized Bed Catalytic Reactors," *Chem. Eng. Sci.*, **24**, 1,351 (1969).

Krambeck, F. J., S. Katz, and R. Shinnar, "A Stochastic Model for Fluidized Beds," *Chem. Eng. Sci.*, **24**, 1,497 (1969).

Ligon, J. R., and N. R. Amundson, "Modeling of Fluidized Bed Reactors—VI(a) An isothermal bed with stochastic bubbles," *Chem. Eng. Sci.*, **36**, 653 (1981).

Mori, S., and C. Y. Wen, "Estimation of Bubble Diameter in Gaseous Fluidized Beds," *AIChE J.*, **21**, 109 (1975).

Mori, S., and C. Y. Wen, "Simulation of Fluidized Bed Reactor Performance by Modified Bubble Assemblage Model," *Fluidization Technology*, V-1, D. L. Kearins, Ed., Hemisphere, Washington, DC (1976).

Nassar, R., et al., "A Stochastic Treatment of Unimolecular Reactions in an Unsteady State Continuous Flow System," *Chem. Eng. Sci.*, **36**, 1,307 (1981).

Nassar, R., J. R. Too, and L. T. Fan, "Simulation of the Performance of a Flow System Consisting of Interconnected Reactors by Markov Processes," *Residence Time Distribution Theory in Chemical Engineering*, A. Pethö and R. D. Noble, Eds., Verlag Chemie, Weinheim, West Germany (1982).

Orcutt, J. C., and B. H. Carpenter, "Bubble Coalescence and the Simulation of Mass Transport and Chemical Reaction in Gas Fluidized Beds," *Chem. Eng. Sci.*, **26**, 1,049 (1971).

Peters, M. H., L. S. Fan, and T. L. Sweeney, "Reactant Dynamics in Catalytic Fluidized Bed Reactors with Flow Reversal of Gas in the Emulsion Phase," *Chem. Eng. Sci.*, **37**, 553 (1982).

Peters, M. H., "The Influence of Flow Reversal of Gas on the Selectivity of Complex Reaction Schemes in a Fluidized Bed," Paper No. 81k, AIChE Ann. Meet., Los Angeles (Nov., 1982).

Manuscript received Jan. 3, 1984; revision received June 25, and accepted July 3.